



NRL/MR/6355--15-9584

Corrosion-Fatigue Cracking in HY-80 and HY-130 Steels

P.S. PAO

R.L. HOLTZ

Multifunctional Materials Branch

Materials Science and Technology Division

January 22, 2015

Approved for public release; distribution is unlimited.

REPORT DOCUMENTATION PAGE				Form Approved OMB No. 0704-0188	
Public reporting burden for this collection of information is estimated to average 1 hour per response, including the time for reviewing instructions, searching existing data sources, gathering and maintaining the data needed, and completing and reviewing this collection of information. Send comments regarding this burden estimate or any other aspect of this collection of information, including suggestions for reducing this burden to Department of Defense, Washington Headquarters Services, Directorate for Information Operations and Reports (0704-0188), 1215 Jefferson Davis Highway, Suite 1204, Arlington, VA 22202-4302. Respondents should be aware that notwithstanding any other provision of law, no person shall be subject to any penalty for failing to comply with a collection of information if it does not display a currently valid OMB control number. PLEASE DO NOT RETURN YOUR FORM TO THE ABOVE ADDRESS.					
1. REPORT DATE (DD-MM-YYYY) 22-01-2015		2. REPORT TYPE Memorandum Report		3. DATES COVERED (From - To) October 2011 – September 2014	
4. TITLE AND SUBTITLE Corrosion-Fatigue Cracking in HY-80 and HY-130 Steels				5a. CONTRACT NUMBER	
				5b. GRANT NUMBER	
				5c. PROGRAM ELEMENT NUMBER	
6. AUTHOR(S) P.S. Pao and R.L. Holtz				5d. PROJECT NUMBER	
				5e. TASK NUMBER	
				5f. WORK UNIT NUMBER 63-2634-A4	
7. PERFORMING ORGANIZATION NAME(S) AND ADDRESS(ES) Naval Research Laboratory 4555 Overlook Avenue, SW Washington, DC 20375-5328				8. PERFORMING ORGANIZATION REPORT NUMBER NRL/MR/6355--15-9584	
9. SPONSORING / MONITORING AGENCY NAME(S) AND ADDRESS(ES) Office of Naval Research One Liberty Center 875 North Randolph Street, Suite 1425 Arlington, VA 22203-1995				10. SPONSOR / MONITOR'S ACRONYM(S) ONR	
				11. SPONSOR / MONITOR'S REPORT NUMBER(S)	
12. DISTRIBUTION / AVAILABILITY STATEMENT Approved for public release; distribution is unlimited.					
13. SUPPLEMENTARY NOTES					
14. ABSTRACT An investigation was carried out to characterize the effects of environment (including [NaCl] concentration) and load ratio on fatigue crack growth kinetics of HY-80 and HY-130 steels. Fracture mechanics wedge-opening-load (WOL) specimens oriented in the longitudinal direction (LT) were used in the current study. The test environments were vacuum, ambient air, and saltwater with [NaCl] concentrations ranging from 0.1 to 15%. Three load ratios, corresponding to $R = 0.1$, $R = 0.5$, and $R = 0.85$, were examined. The results indicate: (1) the fatigue crack growth rates and fatigue crack growth threshold, ΔK_{th} , for HY-80 steel and HY-130 steel are comparable at similar stress ratios in each of the three test environments (vacuum, ambient air, and 1% NaCl solution); (2) in the low stress intensity region, the fatigue crack growth rates of both HY-80 steel and HY-130 steel are higher and ΔK_{th} are lower at a high load ratio than those obtained at lower load ratios; (3) the fatigue crack growth rates of HY-80 steel and HY-130 steel obtained in ambient air and in 3.5% NaCl solution are comparable and are significantly higher than those obtained in vacuum; (4) the fatigue crack growth responses of HY-130 steel are not affected by the change in [NaCl] concentration; and (5) cathodic protection of HY-130 steel in saltwater does not lower its corrosion-fatigue cracking resistance.					
15. SUBJECT TERMS Corrosion-fatigue Environmental effect Steel					
16. SECURITY CLASSIFICATION OF:			17. LIMITATION OF ABSTRACT Unclassified Unlimited	18. NUMBER OF PAGES 28	19a. NAME OF RESPONSIBLE PERSON Peter S. Pao
a. REPORT Unclassified Unlimited	b. ABSTRACT Unclassified Unlimited	c. THIS PAGE Unclassified Unlimited			19b. TELEPHONE NUMBER (include area code) (202) 767-0224

Contents

Introduction	1
Experimental Procedure	1
Results and Discussion	1
HY-80 Steel	1
Effect of Load Ratio	1
Effect of Test Environment	2
HY-130 Steel	3
Effect of Load Ratio	3
Effect of Test Environment	3
Effect of [NaCl] Concentration	3
Effect of Zn-Coupling	3
Comparison of Fatigue Crack Growth Responses of HY-80 Steel and HY-130 Steel in Saltwater	4
Fracture Paths Examination by Electron Backscatter Diffraction (EBSD) Analysis	4
Conclusions	5
References	6
Appendix A – Figures	7

ACKNOWLEDGMENTS

The author gratefully acknowledges the support from Office of Naval Research (ONR), Arlington, VA, monitored by Dr. Lawrence Kabacoff. The author wishes to express his appreciation to Dr. A.K. Vasudevan, formerly with ONR, for his helpful discussions and to Dr. C.R. Feng for his assistance in SEM fractographic examination.

INTRODUCTION

HY-80 and HY-130 steels are quenched and tempered low-carbon alloy steels with minimum tensile strength of 552 MPa (80 ksi) and 896 MPa (130 ksi), respectively. These alloys are extensively used in marine structures and heavy construction equipment because of their high tensile strengths, good ductility and notch toughness, good weldability, low cost, easy fabrication, and well established manufacturing industries. These steels are often exposed to the unique naval environments such as saltwater, salt fog, and near-coastal ocean spray.

A study was conducted to determine the effects of environments (vacuum, ambient air, and saltwater with [NaCl] concentration varying from 0.1 to 15%), and load ratio ($R = 0.1$ to 0.85) on fatigue crack growth kinetics (Stages 1 and 2 and ΔK_{th}) of HY-80 and HY-130 steels. Since these steels are often cathodically protected by Zn-coupling in marine environments, the effect of Zn-coupling on corrosion-fatigue crack growth was also examined. The results are compiled into this report.

EXPERIMENTAL PROCEDURE

Materials used in this study were 12.7 mm-thick HY-80 and HY-130 steel plates.

For fatigue crack growth studies, 12.7-mm-thick, 64.8-mm-wide wedge-opening-load (WOL) fracture mechanics specimens, with crack propagation direction perpendicular to the plate rolling direction (LT), were used. The stress-intensity factor range (ΔK) for the WOL specimens was computed from the relationship (reference 1):

$$\Delta K = [\Delta P/(BW^{1/2})] [(2 + a/W)(0.8072 + 8.858 (a/W) - 30.23 (a/W)^2 + 41.088 (a/W)^3 - 24.15 (a/W)^4 + 4.951 (a/W)^5)/(1 - a/W)^{3/2}], \quad (1)$$

where ΔP = applied load amplitude, B = specimen thickness, W = specimen width, and a = crack length. The fatigue test environments include vacuum ($< 6 \times 10^{-6}$ Pa background pressure), ambient air (20 °C and 42% relative humidity), and in saltwater solution with [NaCl] concentration varying from 0.1 to 15 wt%. In addition, corrosion-fatigue crack growth tests were carried out with and without Zn-coupling. The fatigue crack growth experiments were conducted in accord with ASTM E647 with a cyclic load frequency of 10 Hz, a sine waveform, and load ratios, R , ranging from 0.1 to 0.85. Fatigue crack length and fatigue crack growth rate were continuously monitored by a compliance technique. After fatigue tests, the fatigue-fractured surfaces were studied by scanning electron microscopy (SEM) and electron backscatter diffraction (EBSD) analysis.

RESULTS AND DISCUSSION

HY-80 STEEL

EFFECT OF LOAD RATIO

The effect of load ratio on fatigue crack growth of HY-80 steel in vacuum, ambient air, and 3.5% NaCl solution are shown, respectively, in Figs. A-1a, A-1b, and A-1c. As shown in Fig. A-1, the fatigue crack growth rates above $\Delta K = 10 \text{ MPa}\sqrt{\text{m}}$ at load ratios of 0.1, 0.5, and 0.85 are comparable in each of the test environments. Below ΔK of $10 \text{ MPa}\sqrt{\text{m}}$, the fatigue crack growth rate curves tend to spread out and the fatigue crack threshold stress intensity factor range, ΔK_{th} , is the highest at $R = 0.1$, followed by that at $R = 0.5$, and is the lowest at $R = 0.85$. The fatigue crack growth rate curves obtained in vacuum environment are more compact as the differences among rate curves are small when load ratio varies from 0.1 to 0.85. In more aggressive ambient air and 3.5% NaCl solution, the load ratio effects are more prominent.

The effects of load ratio on ΔK_{th} in three environments are shown in Fig. A-2. As shown in Fig. A-2, in general, the ΔK_{th} decreases with increasing load ratio. The ΔK_{th} at $R = 0.1$ can be as much as twice that at $R = 0.85$ in ambient air and in 3.5% NaCl solution.

EFFECT OF TEST ENVIRONMENT

The effect of test environment on fatigue crack growth of HY-80 steel at $R = 0.1$ and at $R = 0.85$ are shown, respectively, in Figs. A-3a and A-3b. It is interesting to note that the fatigue crack growth rates of HY-80 steel obtained in ambient air and in 3.5% NaCl solution are comparable at similar stress intensities. This indicates that HY-80 steel has good corrosion-fatigue cracking resistance in saltwater environment as there is no further increase in fatigue crack growth rate when test environment changes from ambient air to a “more aggressive” saltwater. Also shown in Fig. A-3, the fatigue crack growth rates are significantly lower and the ΔK_{th} higher in vacuum than those obtained in ambient air and in saltwater.

The effect of test environment on ΔK_{th} of HY-80 steel is shown in Fig. A-2. As shown in Fig. A-2, the ΔK_{th} is highest in inert vacuum environment, followed by in 3.5% NaCl solution, and is lowest in ambient air environment. The reason that ΔK_{th} is slightly higher and the fatigue crack growth rate slightly lower in the near-threshold region in saltwater than those in ambient air can be attributed to the corrosion-product induced wedging phenomenon. The fracture surfaces of HY-80 steel corrode badly in saltwater. The corrosion products, or rust, can accumulate in the crack tip region and wedge open the crack tip during unloading part of the fatigue cycle. This would reduce the effective stress intensity at the crack tip and gives an “apparently higher” ΔK_{th} and lower fatigue crack growth rate in a more aggressive saltwater environment.

Depending on the applied stress intensity, the fatigue crack growth rates of HY-80 steel in ambient air and in saltwater are as much as an order-of-magnitude higher than those obtained in inert vacuum environment, as shown in Fig. A-3. It has been established before that the hydrogen, which is produced as a result of water/steel fracture surface reaction, enters the crack tip region and lowers the fracture stress by hydrogen embrittlement mechanism (references 2 - 5). Because the ambient air fatigue tests are carried out at relative humidity of 42%, the fatigue crack tip region is covered by liquid

water due to capillary condensation. This explains why the fatigue crack growth rates of HY-80 steel in ambient air and in saltwater are comparable in medium and high ΔK regions.

HY-130 STEEL

EFFECT OF LOAD RATIO

The effect of load ratio on fatigue crack growth of HY-130 steel in vacuum, ambient air, and 3.5% NaCl solution are shown, respectively, in Figs. A-4a, A-4b, and A-4c. The general load ratio dependency of HY-130 steel is similar to that of HY-80 steel, and the discussions on Figs. A-1 and A-2 of HY-80 steel can be applied to HY-130 steel, as shown in Figs. A-4 and A-5.

EFFECT OF TEST ENVIRONMENT

The effect of test environment on fatigue crack growth of HY-130 steel at $R = 0.1$ and at $R = 0.85$ are shown, respectively, in Figs. A-6a and A-6b. Again, the environmental response of HY-130 steel is similar to that of HY-80 steel, and the discussions of result on HY-80 steel as shown in Fig. A-3 can be applied here in Fig. A-6. The cause of lower fatigue crack growth rates of HY-130 steel tested in saltwater at $R = 0.1$ in the low stress intensity region when compared to those obtained in ambient air, as shown in Fig. A-6a, can be attributed to corrosion-product induced crack tip wedging as discussed in the previous section.

EFFECT OF [NaCl] CONCENTRATION

The effects of [NaCl] concentration on fatigue crack growth of HY-130 steel at $R = 0.1$ is shown in Fig. A-7. As shown in Fig. A-7, HY-130 steel does not exhibit [NaCl] dependency as the fatigue crack growth responses in 0.1%, 3.5%, and 15% NaCl are identical. In addition, the ΔK_{th} of HY-130 steel in these saltwater environments are also comparable, as shown in Fig. A-8.

EFFECT OF Zn-COUPLING

Because cathodic protection such as Zn-coupling is often applied to steel structures in marine environments, the protected steel structures are cathodic and the hydrogen thus generated can enter the crack tip region. Depending on the material and the amount of hydrogen generated, the load carrying capability of the steel can be significantly compromised by a phenomenon called “hydrogen embrittlement”. Therefore, it is important to establish the effect of Zn-coupling on fatigue crack growth of HY-130 steel, which is often subjected to such “hydrogen embrittlement” conditions.

The effect of Zn-coupling on fatigue crack growth of HY-130 steel at $R = 0.1$ and $R = 0.85$ in 3.5% NaCl solution is shown in Fig. A-9. As shown in Fig. A-9, Zn-coupling has no effect on fatigue crack growth responses of HY-130 steel in 3.5% NaCl solution, at

either low or high load ratios. That is, HY-130 steel is resistant to the “hydrogen embrittlement” condition generated by Zn-coupling.

COMPARISON OF FATIGUE CRACK GROWTH RESPONSES OF HY-80 STEEL AND HY-130 STEEL IN SALTWATER

The fatigue crack growth responses of HY-80 steel and HY-130 steel are compared, at the same load ratios and in the same test environments, in Figs. A-10 through A-12. As shown in these figures, the fatigue crack growth responses of HY-80 steel and HY-130 steel, obtained at similar load ratios and in the same environment, are comparable.

FRACTURE PATHS EXAMINATION BY ELECTRON BACKSCATTER DIFFRACTION (EBSD) ANALYSIS

Because the fracture surfaces of both HY-80 and HY-130 specimens tested in 3.5% NaCl solutions were heavily corroded, the fracture paths under fatigue loading cannot be determined by a conventional SEM analysis. To circumvent this difficulty, EBSD analysis is performed on the crack tip of fatigue cracked specimens with the goal to determine whether the fracture paths are intergranular or transgranular, or both. The results of EBSD analyses on HY80 steel and HY-130 steel are shown in Fig. A-13 through A-16 for various specimens tested at different load ratios and environments. Because the grain sizes of HY-80 and HY-130 are very fine and are only several times larger than the EBSD sampling steps, sometimes it is difficult to determine the fracture paths. Even with this difficulty, the fracture paths in HY-80 steel are predominantly transgranular in both saltwater and vacuum environments. The transgranular nature of the fracture path is particularly evident for HY-80 steel fatigue tested in saltwater as shown in Fig. A-12.

The fatigue fracture paths in HY-130 steel as shown in Figs. A-13 and A-14 are not clear. While some larger-grain areas show transgranular fracture, which is evident in Fig. A-13, yet intergranular separation cannot be ruled out when the crack goes through smaller-grain areas.

CONCLUSIONS

The fatigue crack responses of HY-80 steel and HY-130 steel, obtained at the same load ratio and in the same test environment, are comparable. Their ΔK_{th} under similar conditions are also comparable.

In the low stress intensity region, the fatigue crack growth rates of both HY-80 steel and HY-130 steel are higher and ΔK_{th} are lower at a high load ratio than those obtained at lower load ratios.

The fatigue crack growth rates of HY-80 steel and HY-130 steel obtained in ambient air and in 3.5% NaCl solution are comparable and are significantly higher than those obtained in vacuum. The ΔK_{th} obtained in ambient air and in 3.5% NaCl solution are significantly lower than that obtained in vacuum.

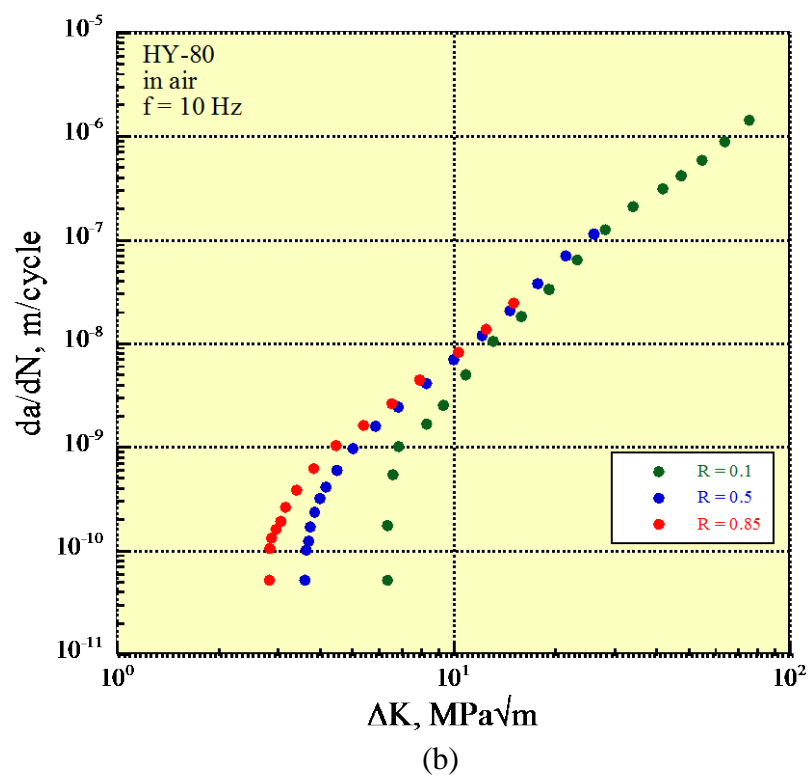
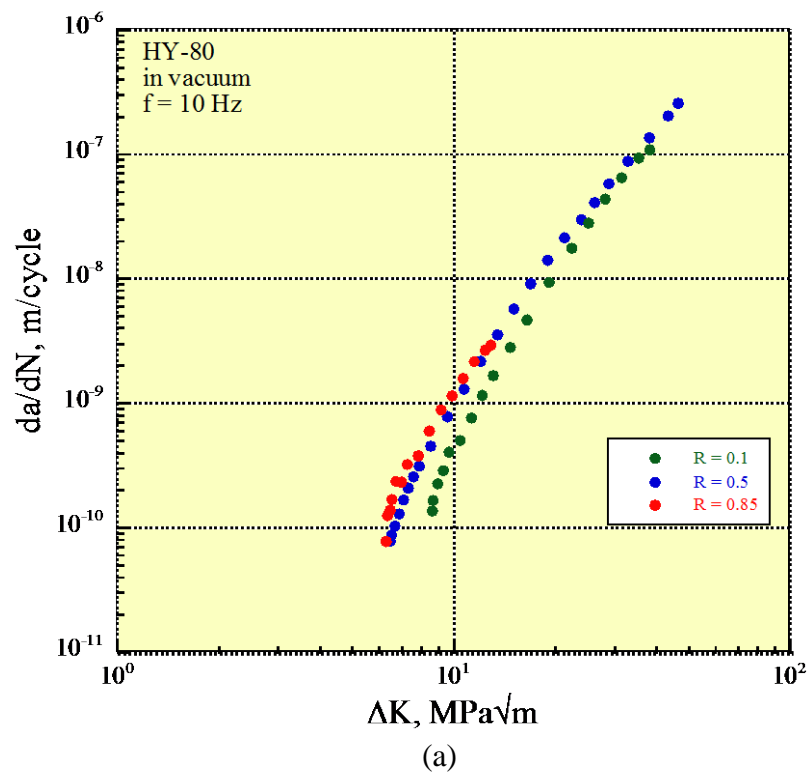
The fatigue crack growth responses of HY-130 steel are not affected by the change in [NaCl] concentration. Fatigue crack growth rates and ΔK_{th} are the same for HY-130 steel fatigue tested in 0.1% and 15% NaCl solutions.

Corrosion-fatigue crack growth responses of HY-130 steel in 3.5% NaCl with and without Zn-coupling are similar. Cathodic protection of HY-130 steel in saltwater does not lower its corrosion-fatigue cracking resistance.

REFERENCES

1. Ashok Saxena and S.J. Hudak, Jr., *Int. J. Fract.*, 1978, Vol. 14, pp. 453-468.
2. G.W. Simmons, P.S. Pao, and R.P. Wei, *Metall. Trans. A*, 1978, Vol. 9A, pp. 1147-1158.
3. H.H. Johnson and A.M. Willner, *Appl. Mater. Res.*, 1965, Vol. 4, p. 43.
4. D.P. Williams and H.G. Nelson, *Metall. Trans. A*, 1970, Vol. 1A, p. 3.
5. S.J. Hudak and R.P. Wei, *Metall. Trans. A*, 1976, Vol. 7A, p. 235.

APPENDIX A FIGURES



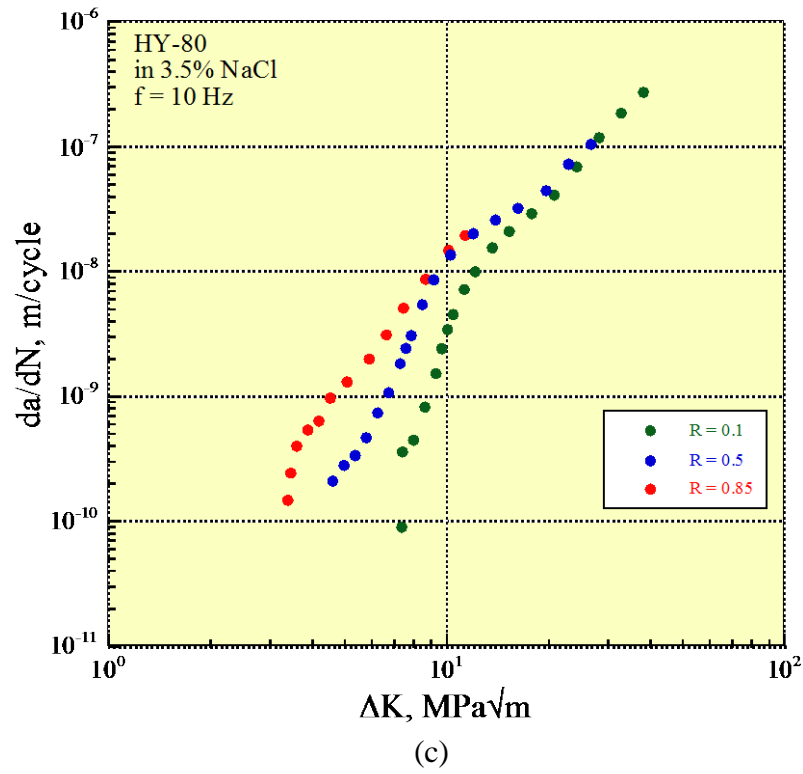


Figure A-1: Fatigue crack growth of HY-80 steel in (1) vacuum, (b) ambient air, and (c) 3.5% NaCl.

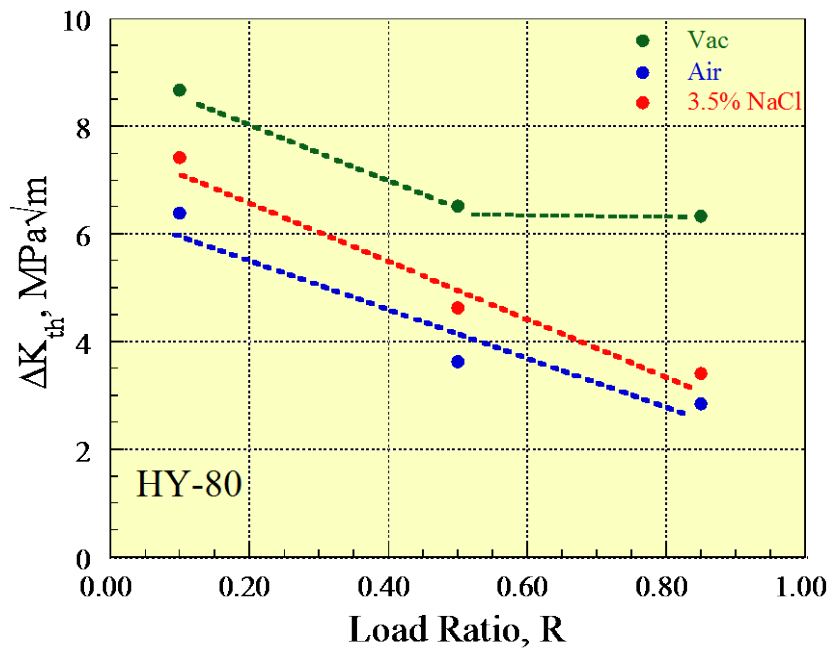


Figure A-2: Effect of load ratio on ΔK_{th} in vacuum, ambient air, and 3.5% NaCl for HY-80 steel.

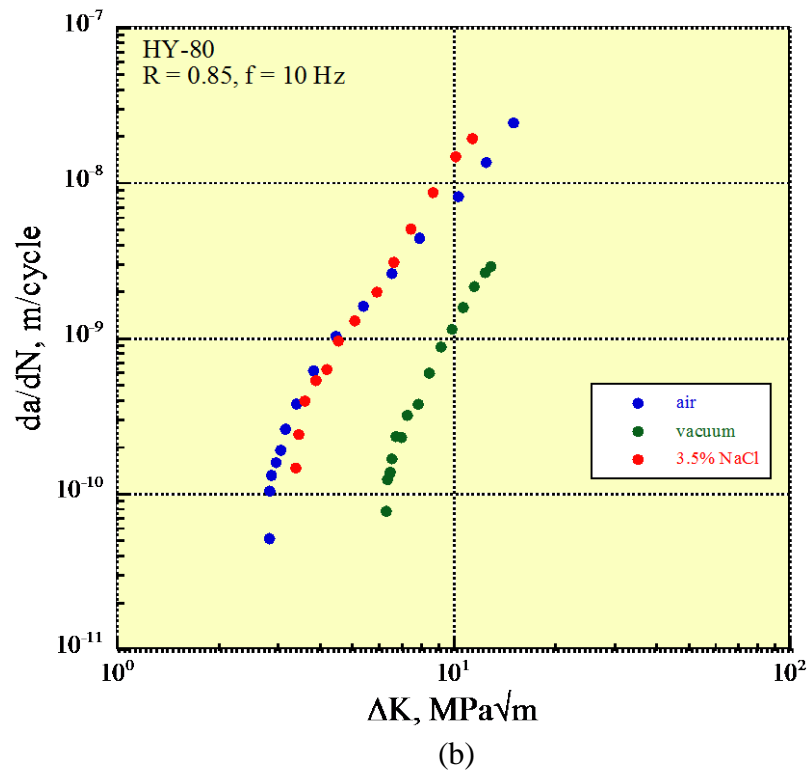
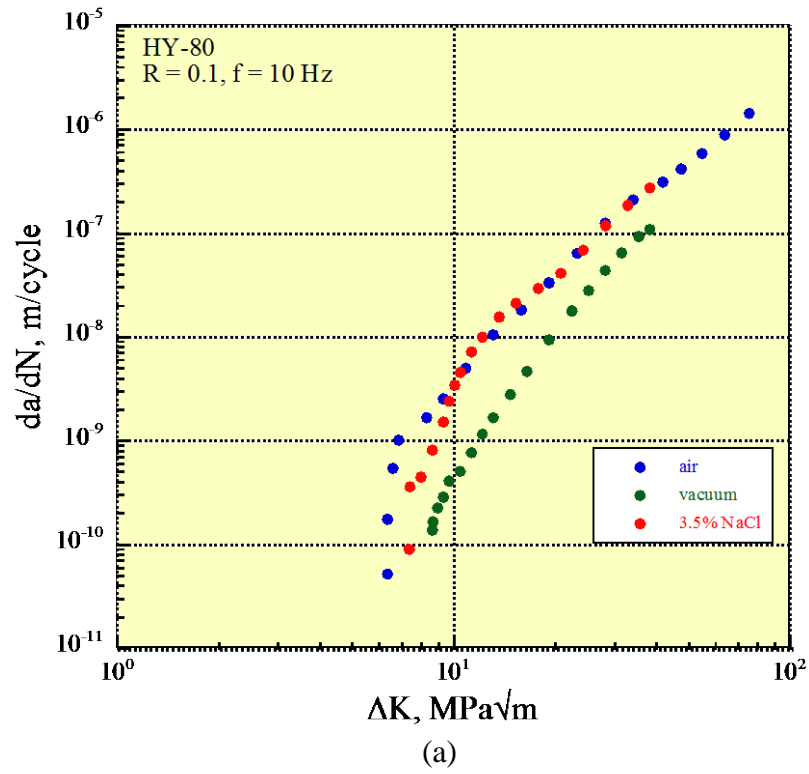
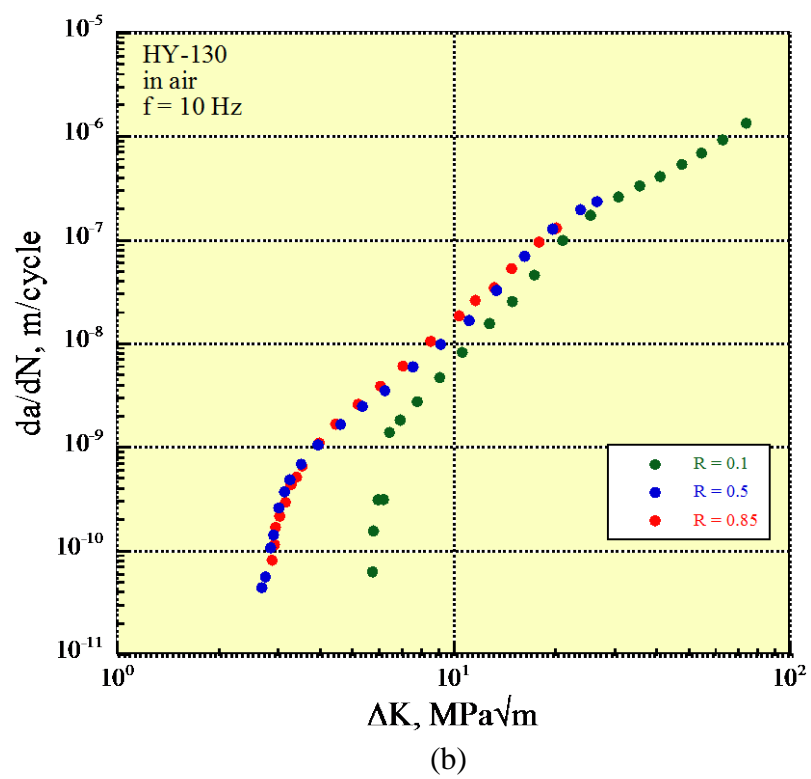
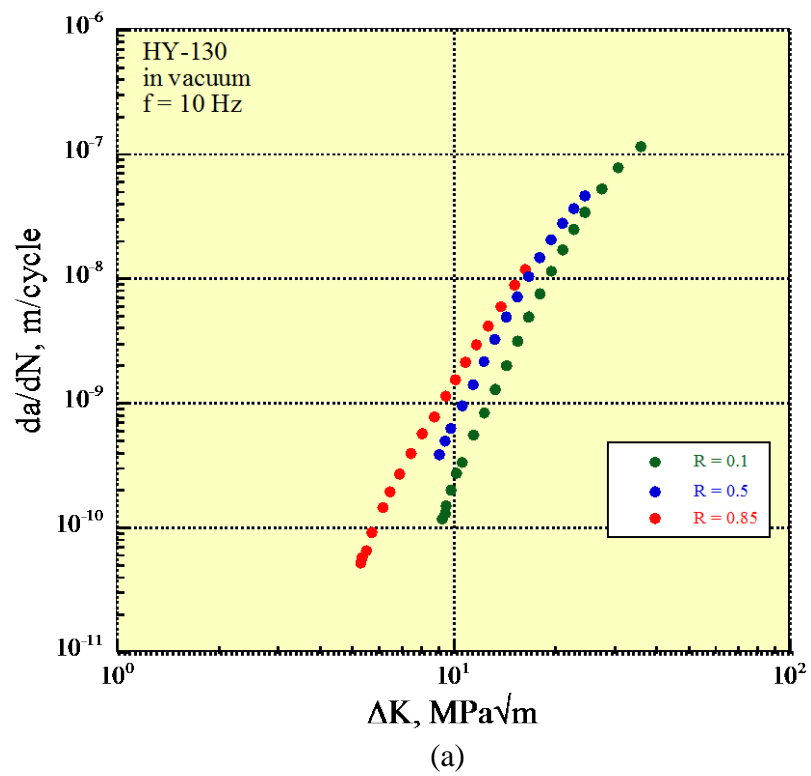


Figure A-3: Effect of environment on fatigue crack growth of HY-80 steel at (a) R = 0.1 and (b) R = 0.85.



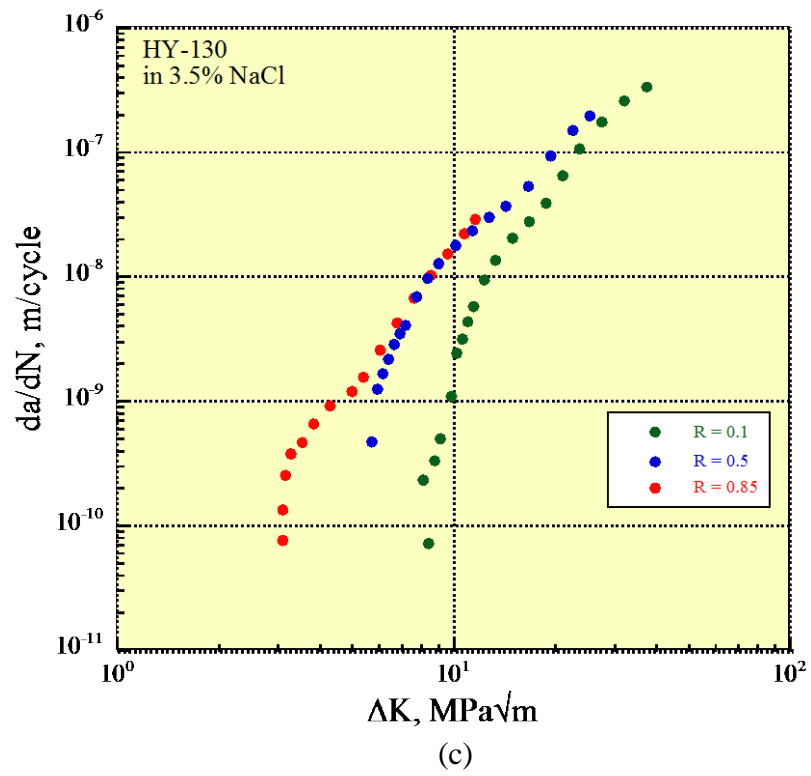


Figure A-4: Fatigue crack growth of HY-130 steel in (1) vacuum, (b) ambient air, and (c) 3.5% NaCl.

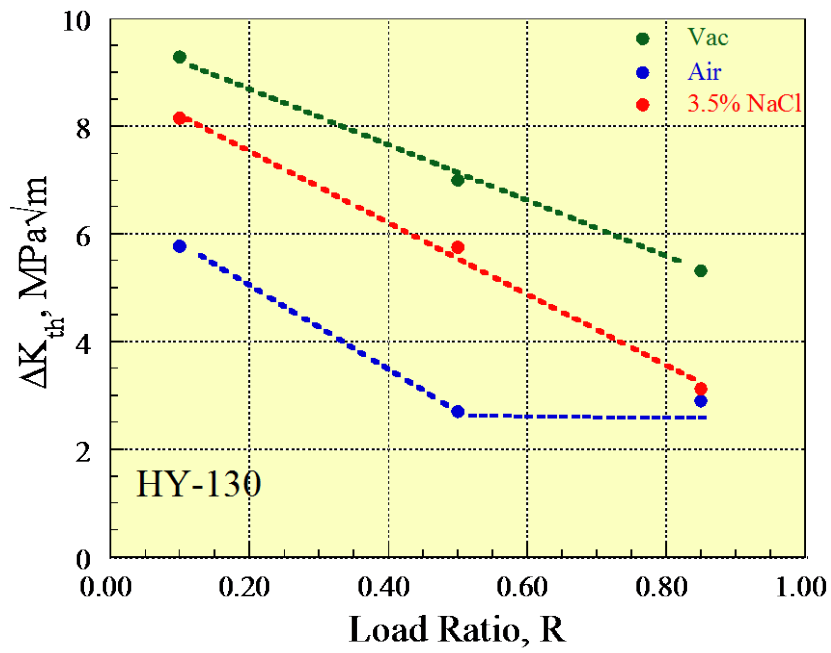


Figure A-5: Effect of load ratio on ΔK_{th} in vacuum, ambient air, and 3.5% NaCl for HY-130 steel.

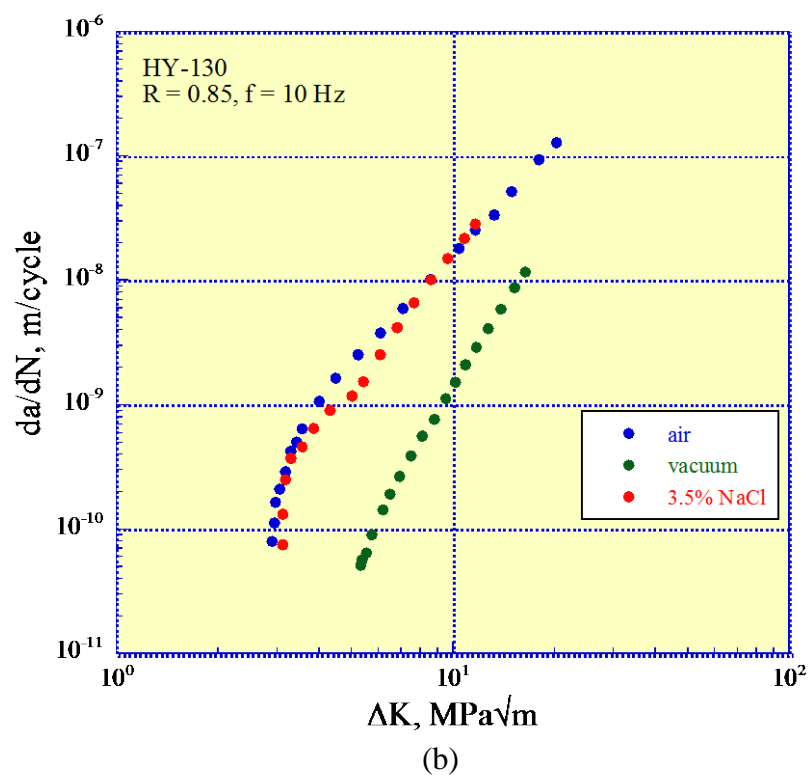
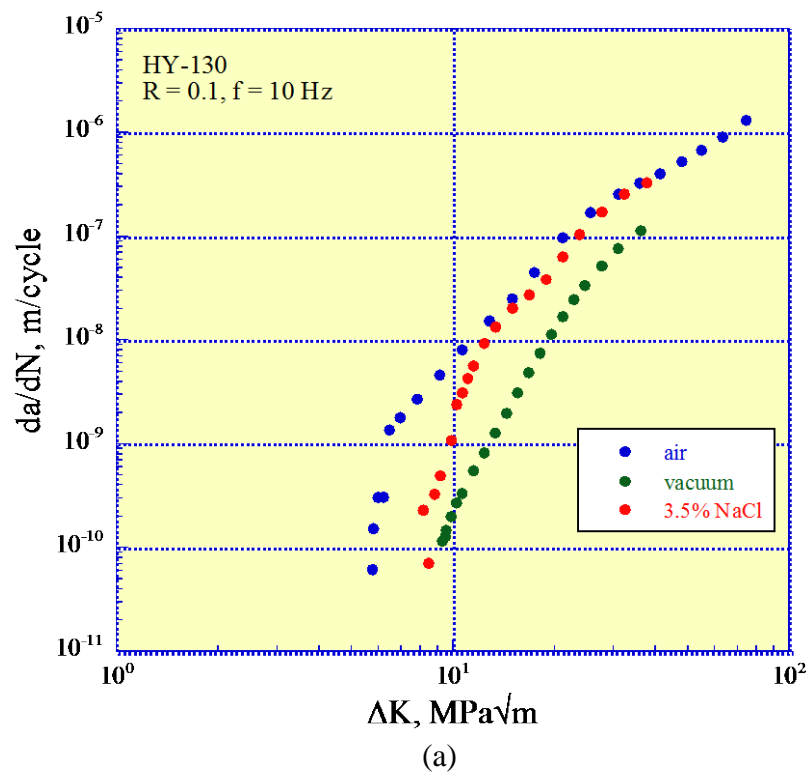


Figure A-6: Effect of environment on fatigue crack growth of HY-130 steel at (a) R = 0.1 and (b) R = 0.85.

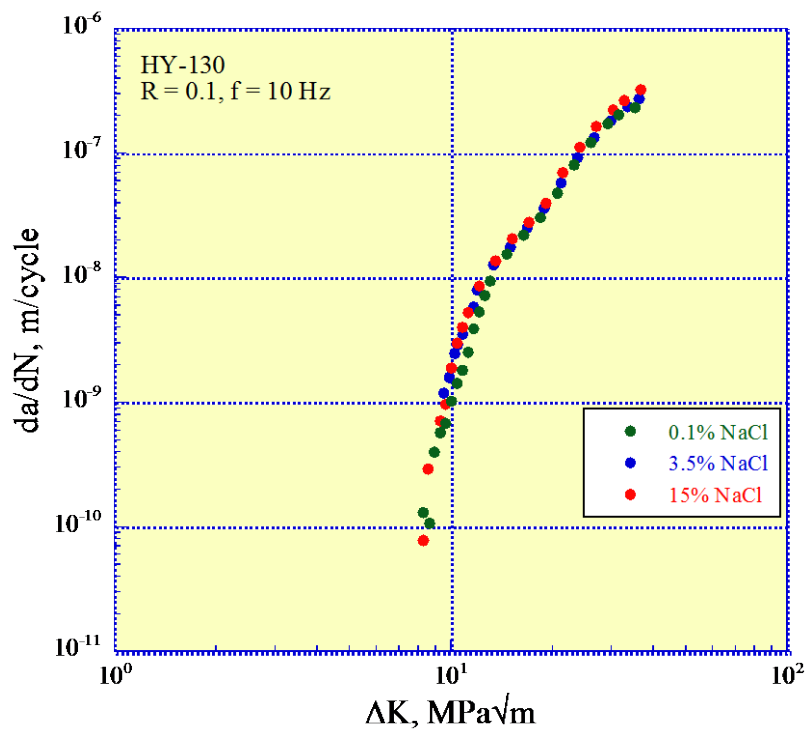


Figure A-7: Effect of [NaCl] concentration on fatigue crack growth of HY-130 steel at R = 0.1.

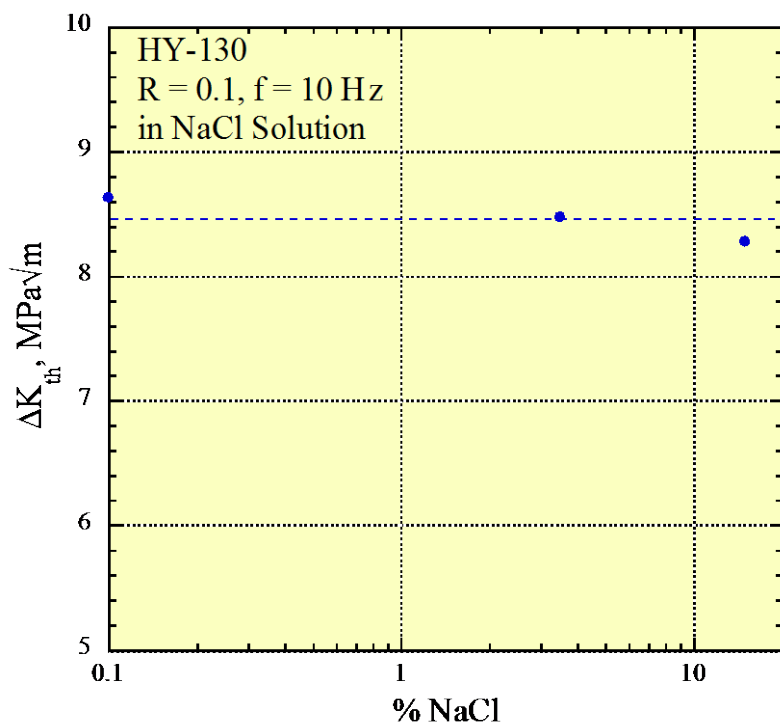


Figure A-8: Effect of [NaCl] concentration on fatigue crack growth threshold, ΔK_{th} , of HY-130 steel at R = 0.1.

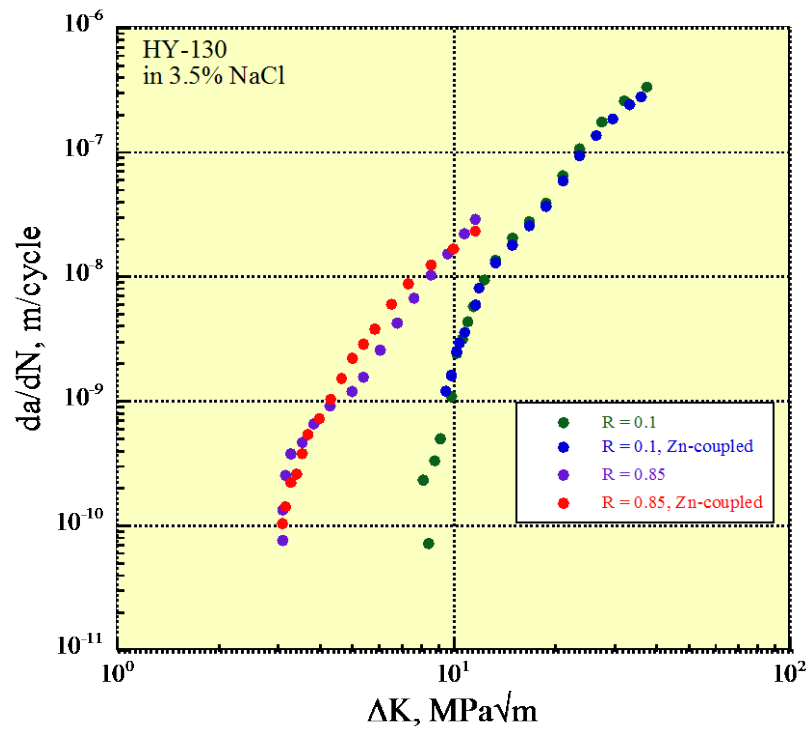


Figure A-9: Effect of Zn-coupling on fatigue crack growth of HY-130 steel in 3.5% NaCl.

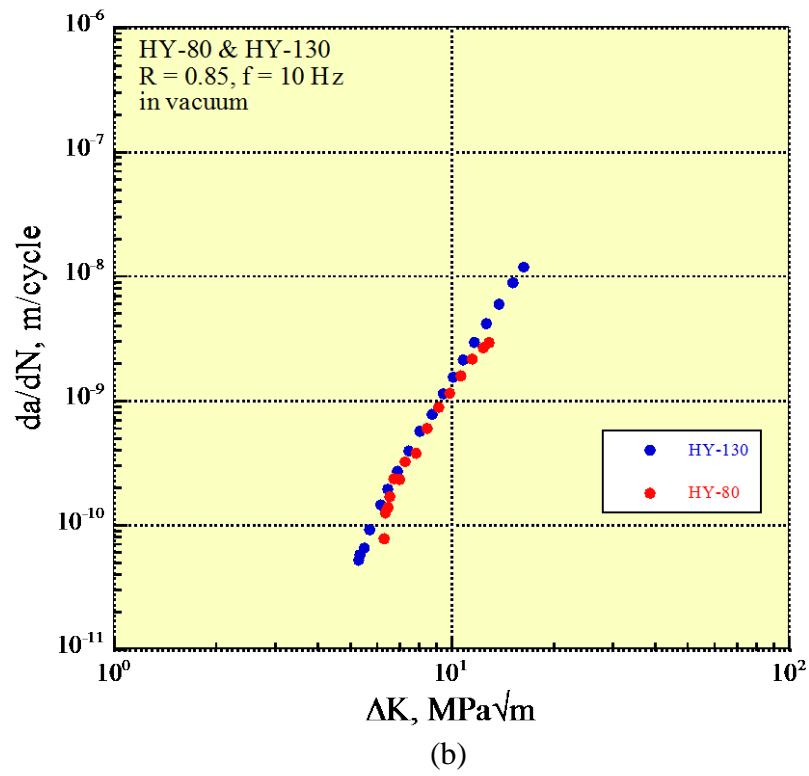
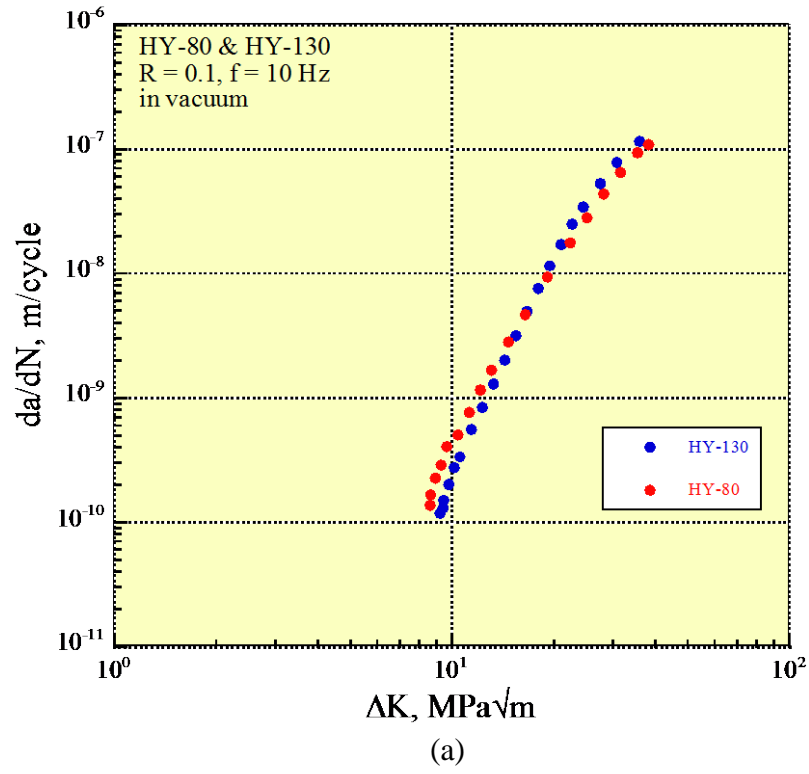


Figure A-10: Comparison of HY-80 and HY-130 fatigue crack growth in vacuum at (a) R = 0.1 and (b) R = 0.85.

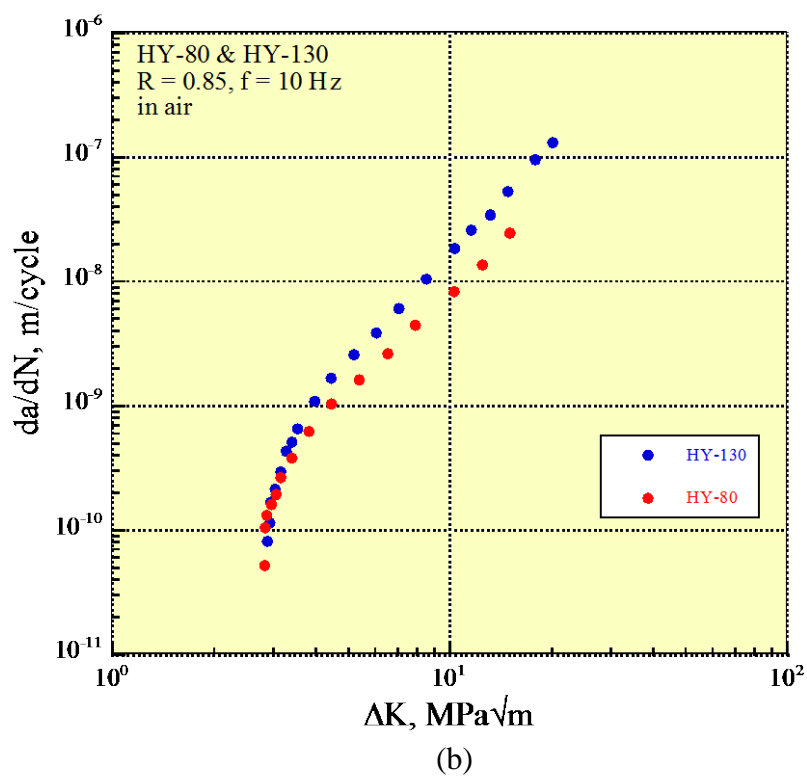
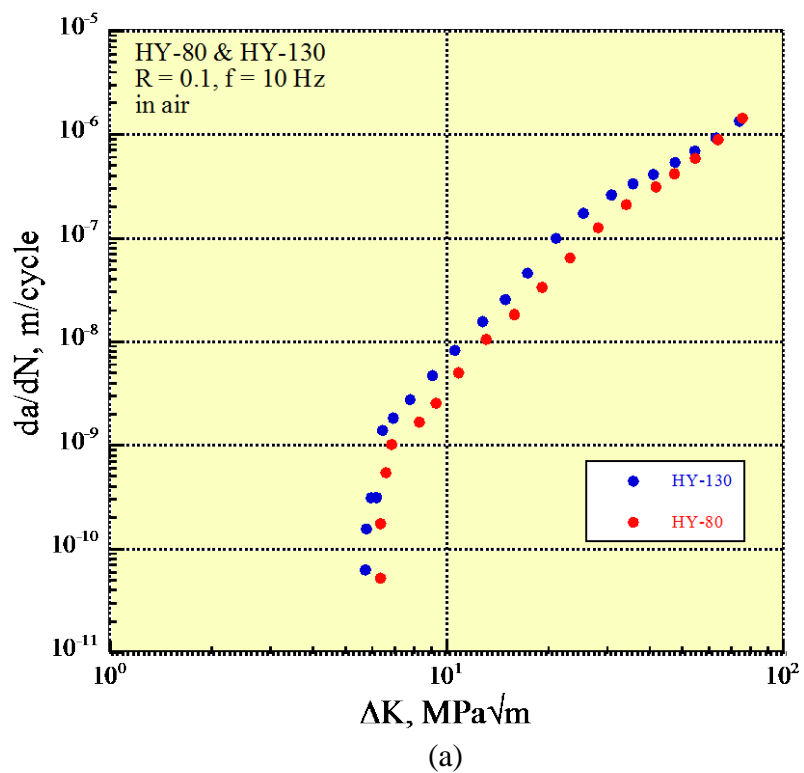


Figure A-10: Comparison of HY-80 and HY-130 fatigue crack growth in air at (a) R = 0.1 and (b) R = 0.85.

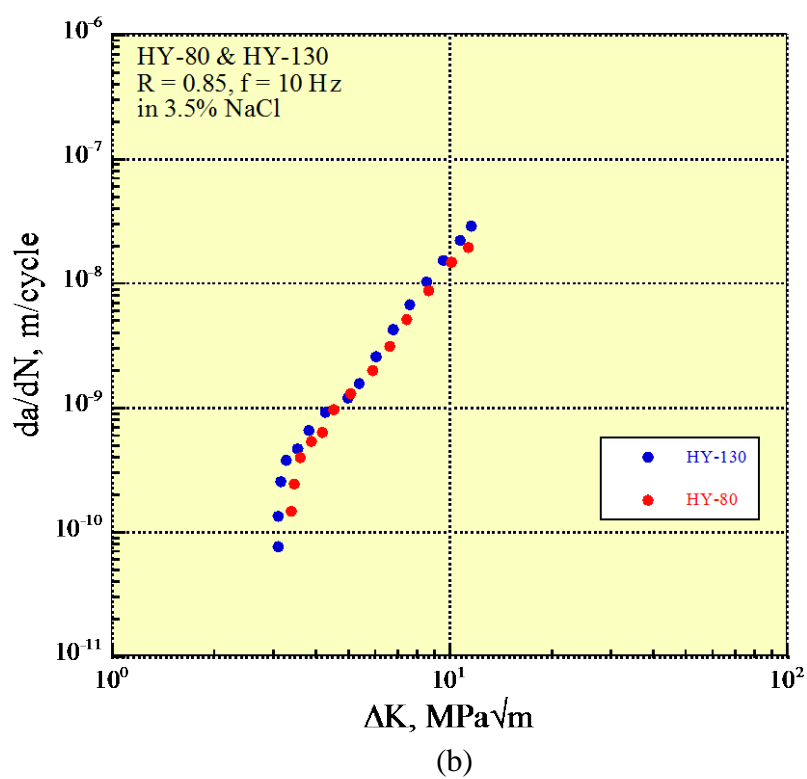
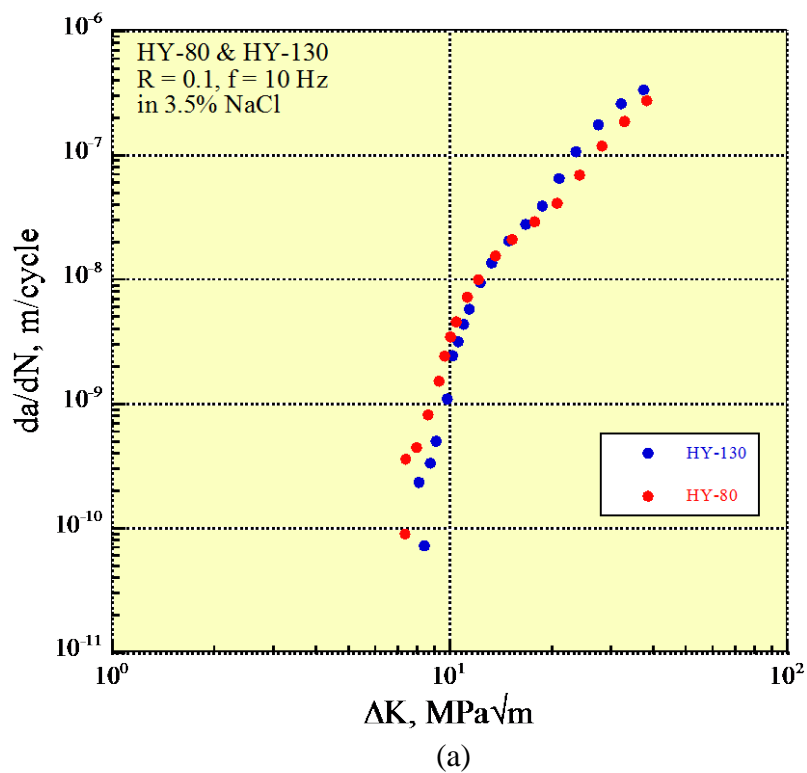


Figure A-10: Comparison of HY-80 and HY-130 fatigue crack growth in 3.5% NaCl at (a) R = 0.1 and (b) R = 0.85.

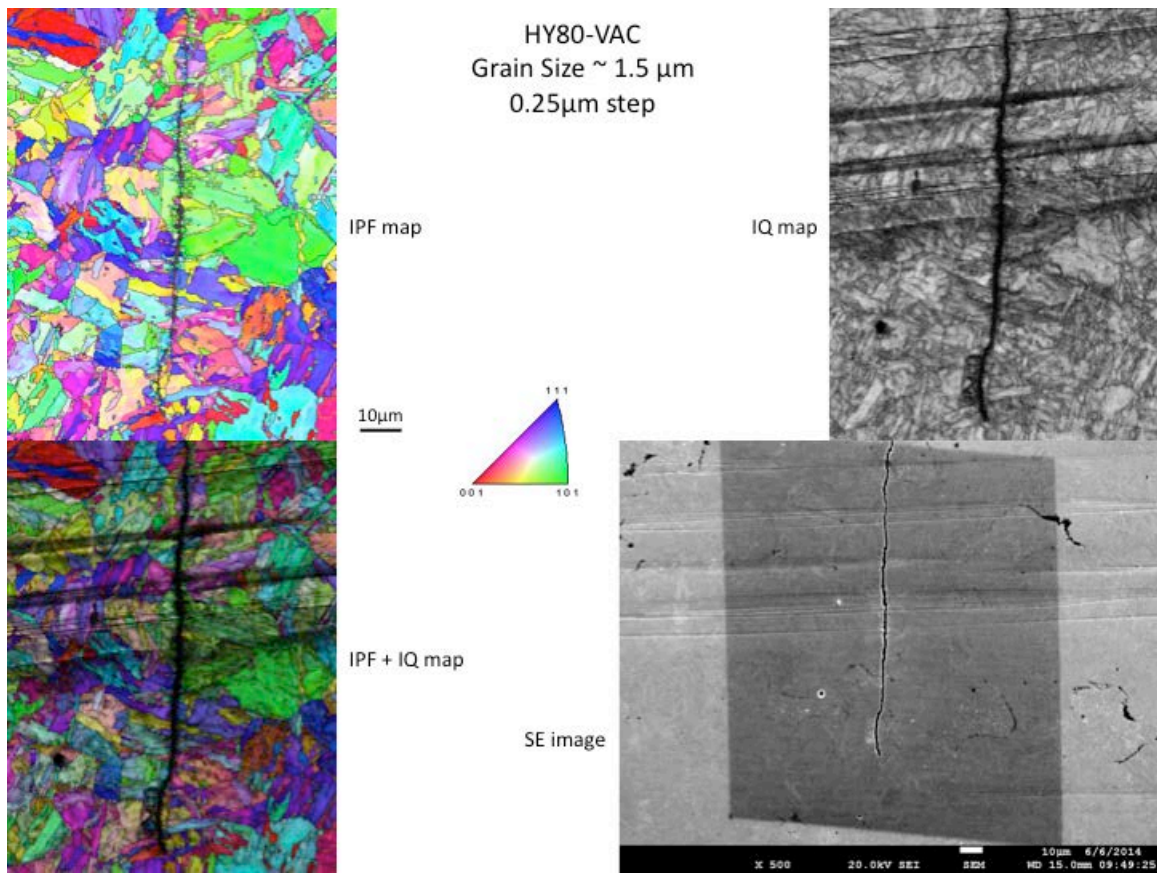


Figure A-11: EBSD and SEM mapping of HY-80 fatigue cracking at $R = 0.1$ in vacuum.

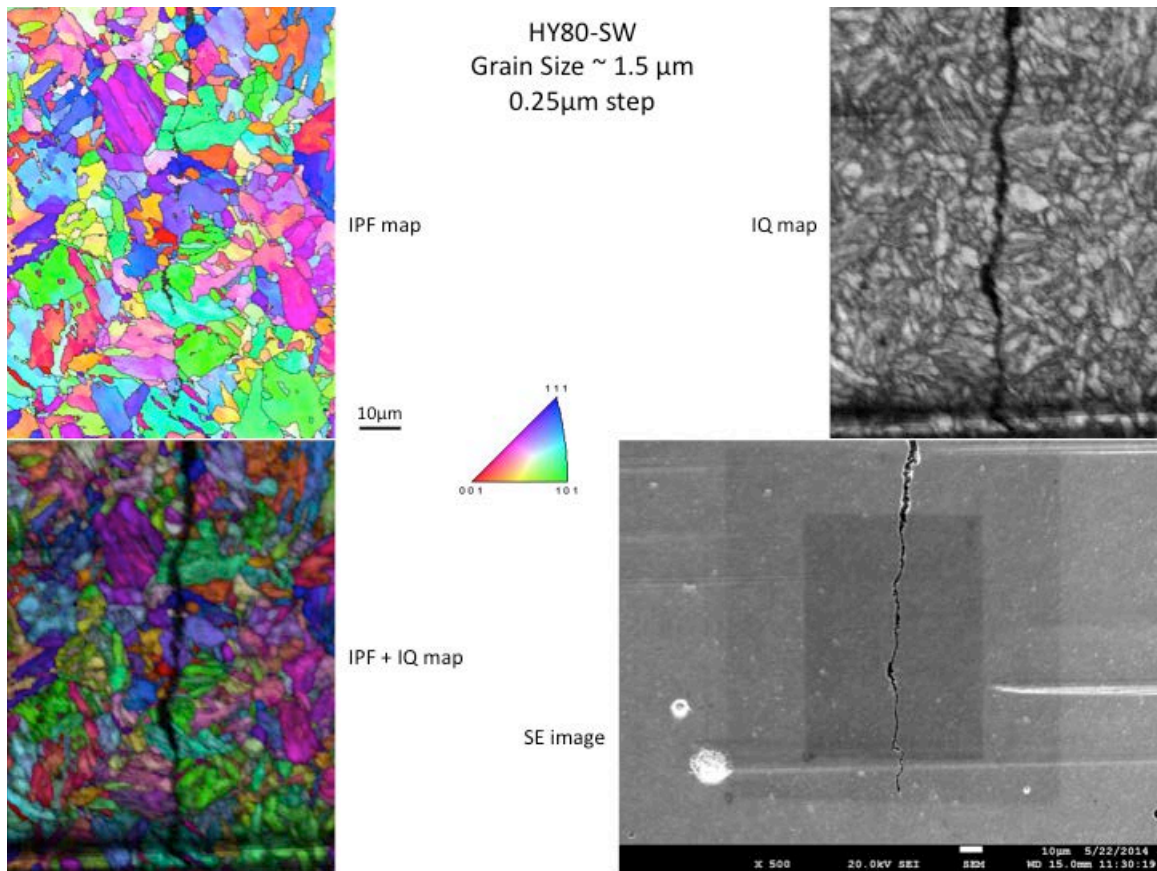


Figure A-12: EBSD and SEM mapping of HY-80 fatigue cracking at $R = 0.1$ in 3.5% NaCl.

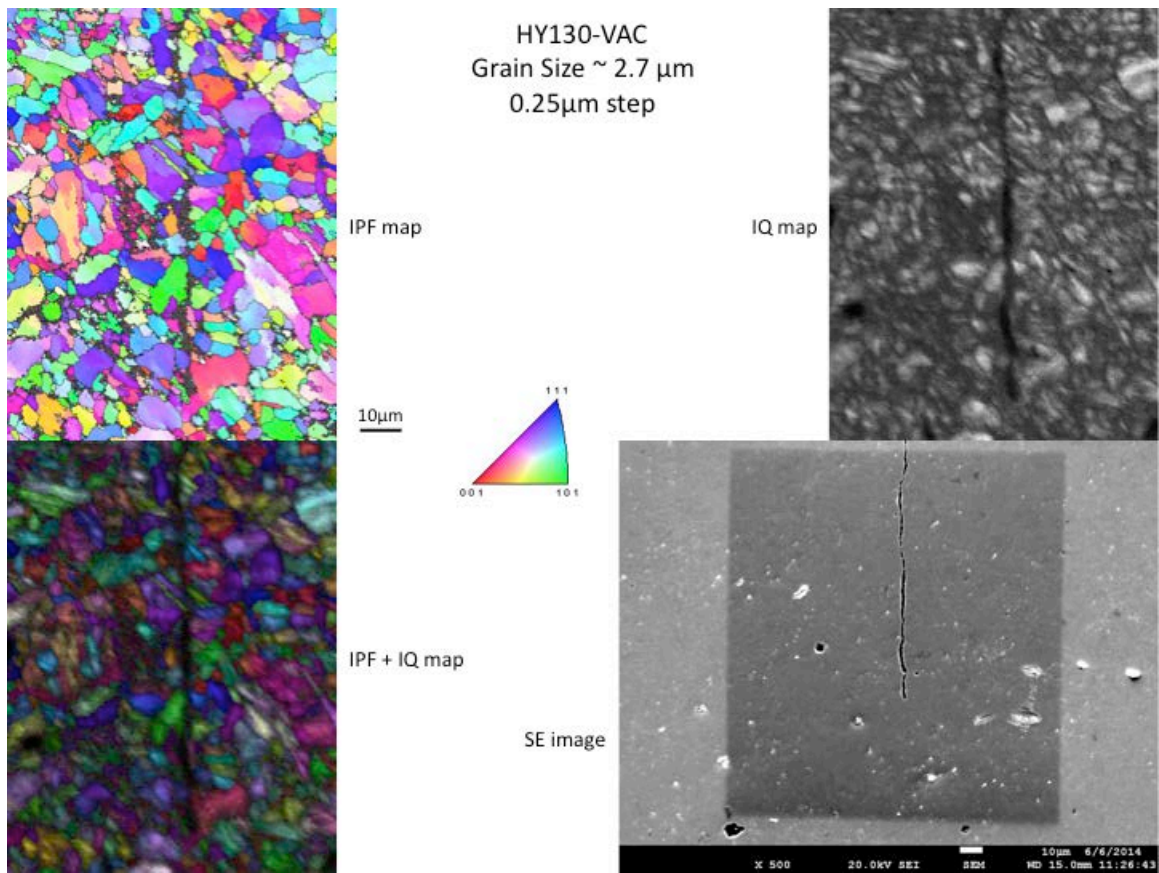


Figure A-13: EBSD and SEM mapping of HY-130 fatigue cracking at $R = 0.1$ in vacuum.

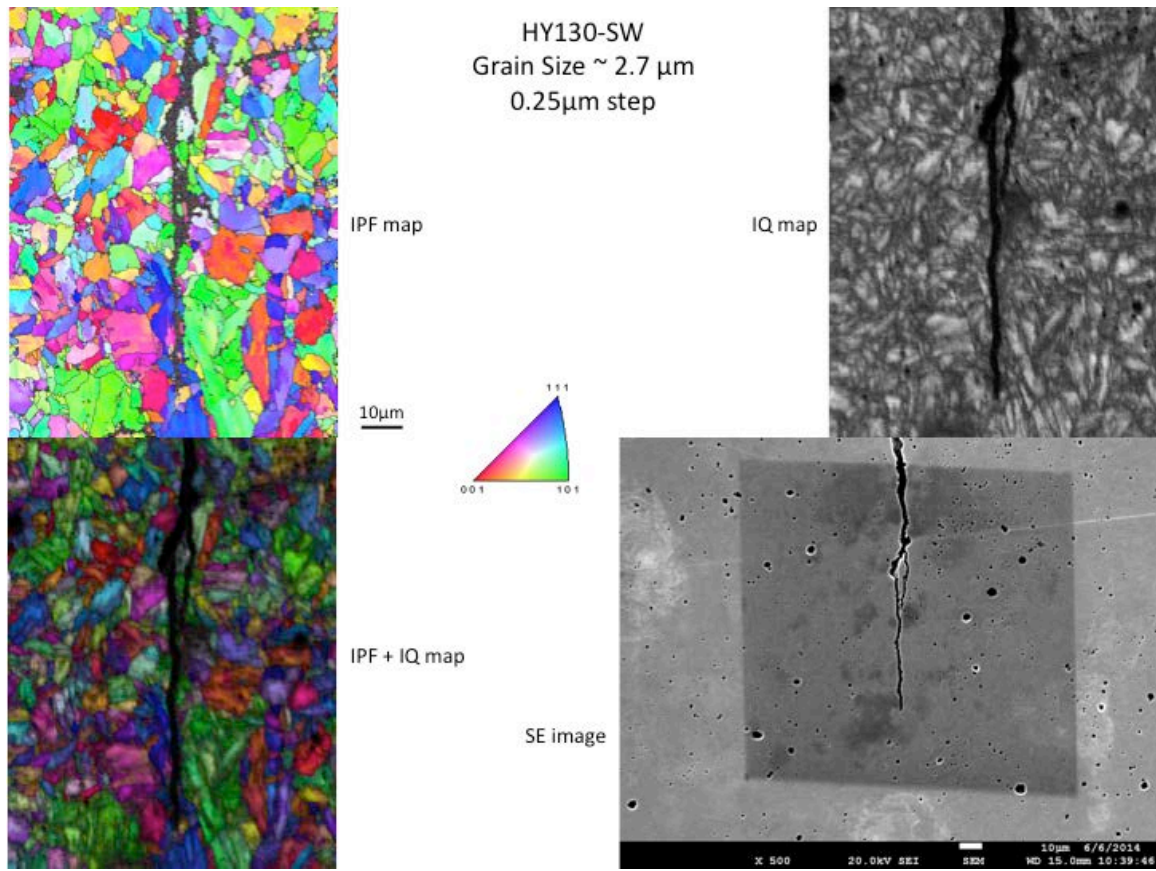


Figure A-14: EBSD and SEM mapping of HY-130 fatigue cracking at $R = 0.1$ in 3.5% NaCl.